Parallel Robot Structure Optimizations for a Friction Stir Welding Application

F. Dardouri[1,2], G. Abba[1] and W. Seemann[2]
[1]*Design, Manufacturing and Control Laboratory (LCFC), Arts et Métiers ParisTech, 57078, Metz, France*
[2]*Institut of Technical Mechanics (ITM), Karlsruhe Institut of Technology-KIT, 76131, Karlsruhe, Germany*

Keywords: Industrial Robot, Friction, Force, Deviation errors, Hybrid Systems, Actuators, Optimization.

Abstract: Today industrial robots are used in many manufacturing applications because of their versatility and easy applicability. Notwithstanding their performance these robots are not suitable for some manufacturing processes where uniform and high forces together with suitable precision of position are required. The present research is focused on one of the high thrust operations, the friction stir welding (FSW). This method for connecting two parts works while the connected materials are in the solid phase. For this reason a very high thrust force is needed to soften the material during the welding process. Due to these high forces the position of the tool of a serial robot deviates from the desired trajectory. In this paper the possibility of using a parallel structure device is investigated to improve the load capacity and stiffness of a heavy manipulator robot. Such a system may exert forces directly on the process tool. In this way the movement of the tool is mainly generated by the industrial serial robot, while the parallel structure ensures the generation of very high thrust forces.

1 INTRODUCTION

Friction Stir Welding process is a comparatively new method of welding. This process invented in 1991 by Wayne Thomas in The Welding Institute (TWI) (Thomas et al., 1991). It enables joining material in solid phase without reaching the melting temperature. Comparing with other joining processes, FSW has many benefits for welding metals. For this reason, after its invention several industries have shown great interest in this process, especially the aerospace industry, mainly due to the exceptional mechanical properties of welds, the absence of defects and typical porosities.

To use this process for welding linear joints, most industrial applications use specified FSW machines. One of the biggest specified machine was developed by ESAB in cooperation with Boeing for the project; space launch system (SLS), of NASA. The first application of FSW in the aeronautics was the Delta II in 1999, (ESAB, 2013). These machines are characterized by high stiffness and thrust capacity, but they require significant investments and have a low manipulapility. It is possible also to use parallel robot (Tricept), see (Smith, 2007). Major research on FSW using parallel structures were developed by HZG in Germany (former GKSS), with a first test in 1998, see (Strombeck et al., 2000). Despite the fact that this type of structure is characterized by a high stiffness but it has a great ability to push only in one direction. To improve the thrust capacity in the other direction of a parallel robot, Palpacelli proposed to join it to a simple cable-driven device whose moving platform was rigidly attached to the robot end-effector. He applied this concept to a tricept after a static and kinematic modeling of the system (Palpacelli, 2016). The application of FSW process using this solution may limit the manipulapility of the structure due to the cables use in the work plane. However, in industry, many applications require a large manipulapility to weld complex joints, demanding machines with several degrees of freedom. Because of that using an industrial robot broadens this flexibility of application.

Of course, Comparing serial robot with many other kinds of machines, they are characterized by low stiffness. For this reason, their use is usually limited to applications like packaging, assembling, or pick and pack, where the positioning accuracy of the tool is not a major factor and a large workspace is required. High force operations like welding or machining are preferably made by machines which have high stiffness, thrust capacity and accuracy, resulting in a better product quality. Nevertheless, their poor flexibility limits many operations, e.g. in cases where a complex

Dardouri, F., Abba, G. and Seemann, W.
Parallel Robot Structure Optimizations for a Friction Stir Welding Application.
DOI: 10.5220/0006434203720381
In *Proceedings of the 14th International Conference on Informatics in Control, Automation and Robotics (ICINCO 2017) - Volume 2*, pages 372-381
ISBN: Not Available

path has to be realized and many places have to be reached by the tool. This flexibility of application is best done by a serial robot. Although In recent years, current researchers tried to replace the dedicated machines by serial robots due to their low cost. The idea in this paper is to use an industrial serial robot to perform the friction stir welding process (FSW).

Due to the high thrust force required for FSW, generally a heavy industrial robot uses to perform the process. Usually, the heavy industrial robots are considered among rigid structures, this condition remains valid unless the forces needed to be created by the robot do not exceed its carrying capacity, which is not the case such as this process requires a very high thrust force that must be provided by the serial robot to hold the contact between the tool and the workpiece surface. For example, to assemble two pieces of aluminum with 6 mm depth, we need 10 kN. For that reason, its positioning accuracy becomes very low, when the effect of transmission elasticity is non-negligible. The deformation of the whole industrial robot needs to be considered especially, for applications that require a precise position of the tool as described by (Soron, 2008) and (Voellner et al., 2007), as in our case, it is necessary that the tool follow a defined trajectory. Therefore, this deformation makes deflection in each joint of the robot, which causes an error in following a given trajectory, see (Strombeck et al., 2000) and affects evidently the quality of the weld. The magnitude of this error depends on the robot position in the work space and the direction of welding (Voellner et al., 2007), (Zaeh and Voellner, 2010) and (Qin et al., 2014). The deviation error can be reduced by solving this difficulty. Several work on manipulator control has been developed to correct the deviation of the robot tool (Yoshikawa, 2000), (Chiaverini et al., 1994), (Raibert and Craig, 1981), et (De Luca et al., 1989). However, there is always a lack of precision, for this reason, in this work, an assistance device has been associated to an industrial robot.

The static performance and the stiffniss of an industrial robot can be greatly improved by adding a device in form of a parallel structure.This assisting device has the architecture of a parallel structure but it is not an existing parallel robot. It is just tree thrust branches able to create together very high thrust forces on the tool which can be controlled easily. In this paper we develop an optimization algorithm to minimize the deviation error. For the first time this algorithm allows the optimization of the parameters defined the parallel structure. In the second time, the optimization of the three forces created by this structure. Thereafter, we simulated the workspace of the whole structure to have an idea about its flexibility of the applications.

2 FSW PROCESS

As shown in Fig. 1 the rotating tool used for the FSW process consists of a probe and a shoulder. Moreover, the external forces exerted on it are the thrust force F exerted by the FSW machine, F_x the axial force during welding when the tool advances along the joint line the material's resistance generates a force along x_0 and Fy, then during tool rotation the flow of material pushes the tool which generates a force along y_0.

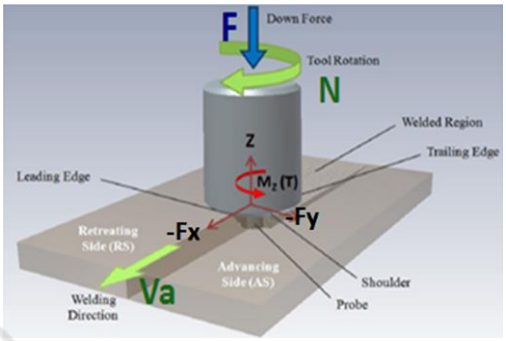

Figure 1: Princible of the FSW Process (Gibson et al., 2014).

FSW is typically described in three steps. The first step is plunging. Here, the probe penetrates into the weld joint between the two parts to be assembled. This step stops when the shoulder touches the surface. The second step is welding. It involves the rotation of the tool and needs a high force which locally softens and mixes the material. This process assists the advance of the tool along the welding line (Fuller 2007, 2007). The third step is retraction; in this step the probe is pulled out vertically from the material.

The FSW process is defined by four parameters, the thrust force F, the welding speed Va, the rotation speed N and the tilt angle B. The force is necessary for maintaining contact between the tool and the pieces to be welded. Further, it softens the material in order to assist the penetration of the probe into the joint. N and Va describe how fast the tool traverses along the interface and rotates, respectively. These two tool speeds have considerable importance, and therefore they need to be correctly set to get a successful welding cycle. There is a relationship between the heat input, the rotation speed and the welding speed during welding. It is arguable that decreasing the lateral speed or increasing the rotation speed will cause a hotter weld. FSW is characterized by a slower Va comparing to other welding processes. The last parameter is B, it tilts the tool mostly between 1.5° and 3.5° degrees such that the front of the tool is higher than the rear. This inclination assists to forge the material. See (Balasubramanian, 2009). To use this pro-

cess, these four parameters must to be set dependly on the material of the parts to be assembled the depth of the joint and the geometry of the tool and its material.

3 THE WRENCH CREATED ON THE PLATFORM

3.1 Description

In the optimization of the deviation error, an industrial robot KUKA KR 500-2MT was used. This is an articulated manipulator with 6 degrees of freedom (DOF) consisting only of revolute joints. This a heavy robot is able to carry in its end a load of 500 kg. Moreover, the first three axes of this robot were modified, such that the transmission are twice as rigid as the transmission of the standard KR 500 Robot. This modification doubles the torque of three motors. However, owing to the high normal force needed for FSW the compliance of the robot remains important and the error due to the deformation in the joints cannot be neglected.

Fig. 2 shows a schematic of the parallel structure that we propose to investigate and which is optimized. The fixed base is connected to the moving platform by three identical limbs. Each limb consists of a prismatic joint P , an universal joint U at point M_i and a spherical joint S at point P_i, for i = 1, 2 and 3. The prismatic joint is driven by actuator which creates a force. Together the three limbs provide an additional force required to minimize the positioning error of the tool. Finally, to summarize This UPS parallel manipulators produces only three forces F_1,F_2 and F_3 on the moving platform but not its actuation and it is controlled in force by retracting or extending the actuators. As shown in the figure r_b is the distance $O_M M_i$ and r_p is the distance $O_6 P_i$.

3.2 Modelling of the System

The reference frame (O_0, x_0, y_0, z_0) is fixed to the ground, the reference frame (O_M, x_M, y_M, z_M) is fixed to the base of the parallel structure while the reference frame (O_6, x_6, y_6, z_6) is moving with the platform. In order to be able to locate the end-effector of an industrial robot, it is necessary to specify its positions and its orientation in the workspace. There are several methods to definie the rotation angles of the transformation between two frames. So in this work to calculate the orientation of the serial robot tool in R_0, the Euler method was used. Three successive rotations are defined as follows:

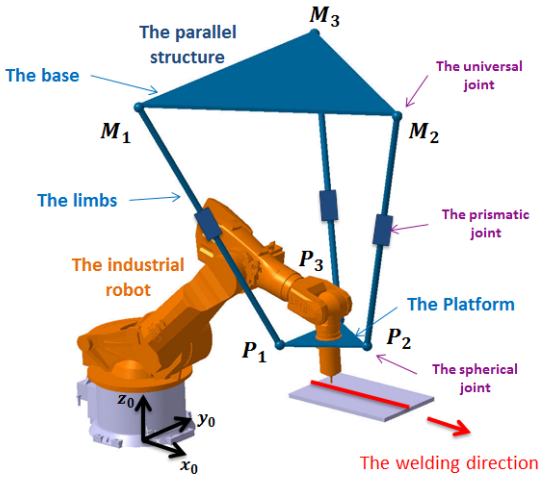

Figure 2: Definition of the parallel structure.

$$R(z_0,A),R(y_0,B),R(x_0,C) \quad (1)$$

The designated angles A, B and C shown in Fig. 3 describe the angles of roll, pitch and yaw. Each new rotation is carried out with respect to one of the fixed frame axes.

C is the rotation around the axis x_0, B is the rotation around the axis y_0 and A is the rotation around the axis z_0. In this work, the orientation of the end-effector is represented to obtain the rotation matrix depending these angles:

$$^0R_6 = \begin{bmatrix} CACB & CASBSC - CCSA & SASC + CACCSB \\ CBSA & CACC + SASBSC & CCSASB - CASC \\ -SB & CBSC & CBCCi \end{bmatrix}$$

Where CA, SA, CB, SB, CC and SC represent cos(A), sin(A), cos(B), sin(B), cos(C) and sin(C) respectively.

The direct geometric model defines the set of relations which express the situation of the object j in the space in terms of the articular variables vector of the robot q.

$$q = \begin{bmatrix} q_1 & q_2 & q_3 & q_4 & q_5 & q_6 \end{bmatrix}^\top \quad (2)$$

q_i is the rotation angle of joint i. The situation of the end-effector j in the frame R_0 is defined by:

$$T = \begin{bmatrix} {}^0P_j & R_j \end{bmatrix}^\top \quad (3)$$

$$T = \begin{bmatrix} x_j & y_j & z_j & A_j & B_j & C_j \end{bmatrix}^\top \quad (4)$$

There are several conventions to calculate these relations. Modified Denavit-Hartenberg (MDH) is usually used to model robots consisting of revolute or

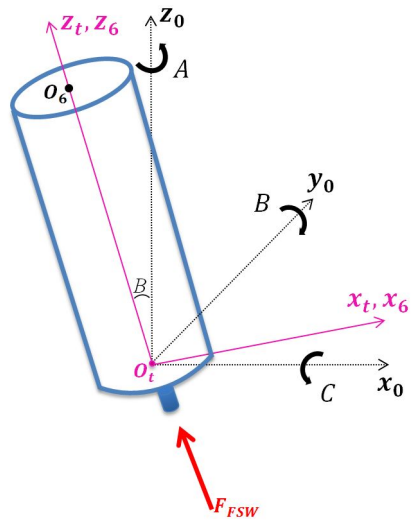

Figure 3: Cordinite to define the tool orientation.

prismatic joints including the manipulator used in this research work. The MDH parameters defined for this robot and are used thereafter with the support of the software SYMORO+ (Khalil and Creusot, 1997) to determine the relationship:

$$T = f(q)\ i \in [1...6] \tag{5}$$

Where x_6, y_6 and z_6 of the equation (4) represent the coordinates of the point O_6 in the fixed frame R_0. This point was noted by:

$${}^0P_6 = \begin{pmatrix} x_6 \\ y_6 \\ z_6 \end{pmatrix}$$

Then the transformation matrix of the end-effector in R_0 is given as :

$${}^0T_6 = \begin{bmatrix} {}^0R_6 & {}^0P_6 \\ 0 & 1 \end{bmatrix}$$

The FSW tool is in direction of the 6th axis of the manipulator with the same orientation of the frame R_6, The position of O_t is

$${}^6P_t = \begin{pmatrix} 0 \\ 0 \\ L_t \end{pmatrix}$$

Where L_t is the length of the tool, see Fig. 3.

$${}^0P_t = {}^0P_6 + {}^0R_6 \begin{pmatrix} 0 \\ 0 \\ L_t \end{pmatrix}$$

And the transformation matrix of the tool in R_0 is :

$${}^0T_t = \begin{bmatrix} {}^0R_6 & {}^0P_t \\ 0 & 1 \end{bmatrix}$$

To calculate the vector P_iM_i it is necessary to calculate first the contact position between the platform and limbs P_i and the contact position between limbs and the fixed base of the parallel structure M_i in the fixed frame R_0 of the industrial robot. As shown in Fig. 4, the orientation of the frame of the parallel structure is the same as of the fixed frame R_0 of the robot. The coordinates of point O_M in the robot frame are $x_M$in x_0, $y_M$in y_0 and H in z_0 direction. Then its position is defined by:

$${}^0P_M = \begin{pmatrix} x_M \\ y_M \\ z_M \end{pmatrix}$$

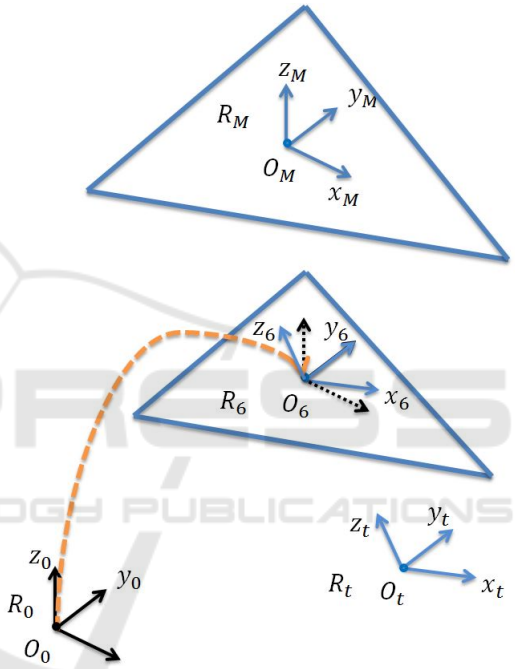

Figure 4: Frames of the robot, the parallel structure and the tool.

Therefore, the transformation matrix of the base of the parallel structure is given by:

$${}^0T_M = \begin{bmatrix} I_3 & {}^0P_M \\ 0 & 1 \end{bmatrix}$$

According to the geometry of the chosen base shown in Fig. 2, the coordinates of point M_i in frame R_M is expressed by:

$${}^MP_{M_1} = \begin{bmatrix} -\frac{r_M}{2} & -\frac{\sqrt{3}}{2}r_M & 0 \end{bmatrix}^\top$$

$${}^MP_{M2} = \begin{bmatrix} r_M & 0 & 0 \end{bmatrix}^\top$$

$${}^MP_{M_3} = \begin{bmatrix} -\frac{r_M}{2} & \frac{\sqrt{3}}{2}r_M & 0 \end{bmatrix}^\top$$

The three contact positions between limbs and the base of the parallel structure in the fixed frame R_0 were defined by:

$$M_i = {}^0P_{M_i} + I_3\,{}^MP_{M_i} \tag{6}$$

The coordinates of the point P_i in frame R_6 are given by:

$${}^6P_{p_i} = \begin{pmatrix} x_{p_i} \\ y_{p_i} \\ z_{p_i} \end{pmatrix}$$

Such as the platform geometry was chosen like the base geometry, for this reason the coordinates of the points expressed in the end-effector frame R_6 are:

$${}^6P_{p_1} = \begin{bmatrix} -\frac{r_p}{2} & -\frac{\sqrt{3}}{2}r_p & 0 \end{bmatrix}^\top$$

$${}^6P_{p_2} = \begin{bmatrix} r_p & 0 & 0 \end{bmatrix}^\top$$

$${}^6P_{p_3} = \begin{bmatrix} -\frac{r_p}{2} & \frac{\sqrt{3}}{2}r_p & 0 \end{bmatrix}^\top$$

To calculate the contact positions between limbs and the platform p_i in the fixed frame R_0 the homogeneous transformation is defined by:

$$P_i = {}^0P_6 + {}^0R_6\,{}^6P_{p_i} \tag{7}$$

As mentioned, in this work the industrial robot allows to move and to position the tool while the parallel structure allows to improve its stiffness. Then, to correct the deviation of the end effector, we need to calculate torques created by the parallel structure on the platform. Each thrust limb of this parallel structure produces a wrench τ_i on the moving platform in point P_i defined by:

$$\tau_i = \left[F_i^\top C_i^\top\right]^\top \tag{8}$$

As shown in Fig. 2 the forces exerted by the limbs are:

$$F_i = f_i\,Z_i \tag{9}$$

f_i is the force created by the actuator i of the parallel structure according to the direction Z_i. According to the transformation matrices expressed in equations (6) and (7), it is possible to calculate the positions of the points P_1, P_2, P_3, M_1, M_2, M_3 during the movement of the industrial robot and for all these configurations in the space. Using the coordinates of these points expressed in the frame R_0 the vector Z_i is obtained as

$$Z_i = \frac{P_iM_i}{\|P_iM_i\|} \tag{10}$$

The vector of moment Ci created by the actuator i in point O_6 is:

$$C_i = O_6P_i \times F_i \tag{11}$$

O_6P_i is the vector from the origin of the coordinate of the platform center defined to the point where the force is exerted

$$O_6P_i = r_pU_{Pi} \tag{12}$$

where r_p is the distance between O_6 and P_i along the direction U_{Pi}.

$$U_{Pi} = \frac{O_6P_i}{\|O_6P_i\|} \tag{13}$$

The spindle of the FSW tool is located at the 6th axis of the manipulator, which is supposed to remain inclined with the small tilt angle M during the process, fig. 3. The FSW force is exerted on the robot tool along its axis z_t as shown in fig. 3. This force can be defined in frame R_0 by:

$$F_{FSW} = \begin{pmatrix} -F_{FSW}sin(B) \\ 0 \\ F_{FSW}cos(B) \end{pmatrix}$$

The wrench at point O_6 created by the FSW force expressed in the fixed frame is:

$$\tau_{FSW} = \begin{bmatrix} -F_{FSW}sin(B) & 0 & F_{FSW}cos(B) & 0 & 0 & 0 \end{bmatrix}^\top \tag{14}$$

Here, we neglet the torque created by the FSW force on the robot tool C_{FSW}.

The total wrench applied on the platform at its center O_6 in the fixed frame R_0 is:

$$F_{ext} = \tau_{FSW} + \sum_{i=1}^{3}\tau_i \tag{15}$$

4 DEVIATION ERROR

This paper presents an approach to improve the quality of friction stir welding using serial robot. The idea is to minimize the deviation error of the tool due to the application of the external forces. The positioning accuracy is depending on the tool orientation and location (Deblaise et al., 2006).

4.1 The Error in the Joint Space

In the industrial robot flexibility is originated from links and joints. However, many researchers claim that, because of the larger stiffness in links, its flexibility could be ignored. (Dumas, 2011) had analysed in her research work that link flexibilities contribute to 25% of the global deflection. For this reason, it is generally admitted that in this kind of machine the flexibility of the structure originates mainly from the joints. The error in the joint space is typically associated to the gearbox flexibility, including motors and

transmissions. This source of rotation is the most important contributor to positional inaccuracies (Duelen and Schröer, 1991), (Schröer, 1993). Therefore, the links of serial robots used in this work are condidered as rigide and only the joint errors are considered, and they are modelled by linear torsional springs (Bres et al., 2010):

$$\tau = K\Delta q \tag{16}$$

Then, τ is the vector of joint torques, and K is a diagonal matrix for the joint stiffness. The difference $\Delta q = (q_d - q)$ is the source of errors in the joint space, where q_d is the desired angle and q is the actual angle. During the application of a load, this model is used to calculate the deformation created in the joints of the robot.

Dynamic model

Dynamic modeling of the robot is required for mechanical design, controls and simulations. A corresponding model shows the relationship between positions of the manipulator joint, torques, speeds, accelerations, friction and external forces. This leads to a set of nonlinear differential equations of order two. It gives the state of the robot at each moment as it can analyse the stability of the control and performance trajectory. The Euler-Lagrange formulation for the joint space dynamic model is written as follows (Khalil and Kleinfinger, 1986) , (Wernholt and Östring, 2003):

$$D(q)\ddot{q} + C(q,\dot{q})\dot{q} + F_v\dot{q} + F_s sgn(\dot{q}) + G(q) = \tau - \tau_{ext} \tag{17}$$

$D(q)$ is the robot inertia matrix, $C(q,\dot{q})\dot{q}$ represents Coriolis and centrifugal terms, F_v is the viscous friction matrix, F_s is the static friction matrix, $G(q)$ is the gravitational torque vector, $J^\top \tau_{ext}$ is wrench vector due to force and torque on the end effector.

During FSW the welding speed Va is always constant and very low, for this reason the acceleration can be assumed to be zero. In this contribution, we use a KuKa robot, which is characterized by a small static friction, and therefore F_s was neglected. Equation (17) can be reduced to equation (18)

$$\tau = G(q) + \tau_{ext} \tag{18}$$

4.2 The Error in the Operational Space

Using the direct kinematic model the relationship between the error in the joint and in the operational spaces can be written as follows:

$$\Delta X = J(q)\Delta q \tag{19}$$

Where $J(q)$ is a 6×6 matrix which is known as a manipulator Jacobian that relates Cartesian velocities to joint velocities.
this jacobian matrix is composed of two parts:

$$J(q) = \begin{pmatrix} J_v \\ J_w \end{pmatrix}$$

J_v calculates the cartesin velocity vector which is obtained from the derivation of the platform position vector

$$J_v = \frac{d^0 P_t}{dq_i} \tag{20}$$

$$J_v = \begin{bmatrix} \frac{dx_6}{dq_1} & \frac{dx_6}{dq_2} & \cdots & \frac{dx_6}{dq_6} \\ \frac{dy_6}{dq_1} & \frac{dy_6}{dq_2} & \cdots & \frac{dy_6}{dq_6} \\ \frac{dz_6}{dq_1} & \frac{dz_6}{dq_2} & \cdots & \frac{dz_6}{dq_6} \end{bmatrix}$$

J_w calculates the vector of rotation speed of the tool that is obtained by this expression:

$$J_w = T_r \frac{dR_t}{dq_i} \tag{21}$$

T_r is a 3×3 matrix defined in (Siciliano and Khatib, 2016)

$$T_r = \begin{bmatrix} -SB & 0 & 1 \\ CBSC & CC & 0 \\ CBCC & -SB & 0 \end{bmatrix}$$

Now combining (16) and (19) provides:

$$\Delta X = JK^{-1}\tau \tag{22}$$

Equations (18) and (22) provide the deviation error in the operational space:

$$\Delta X = JK^{-1}(G(q) + \tau_{ext}) \tag{23}$$

Among the applications of the Jacobian matrix is to define a linear relationship between the external forces exerted at the tool and torques required at the joints of the industrial robot to support these forces. But we cannot use the same Jacobian matrix calculated in the point because the forces exerted on the patform in the point. For this reason, it is necessary to calculate the jacobien in O_6

$$\tau_{ext} = J_6^\top F_{ext} \tag{24}$$

This expression allows to project all end-effector forces at the joints. This important relationship not just for the development of static forces but also can be used for robot control. But we cannot use the same Jacobian matrix calculated in point O_t because the forces were applied to the platform and not to the welded parts. For this reason, it is necessary to calculate the new Jacobian in O_6

$$J_6(q) = \begin{pmatrix} J_{v_6} \\ J_{w_6} \end{pmatrix}$$

R_6 and R_t have the same orientation what gives us this equality

$$J_{w_6} = J_w \tag{25}$$

But,

$$J_{v_6} = \frac{d^0 P_6}{dq_i} \tag{26}$$

Integrating equation (15) in (24) and equation (24) in equation (23) provides:

$$\Delta X = JK^{-1}(G(q) + J_6^{\top}(\tau_{FSW} + \sum_{i=1}^{3} \tau_i)) \tag{27}$$

$$\Delta X = \begin{pmatrix} \Delta x \\ \Delta y \\ \Delta z \\ \Delta C \\ \Delta B \\ \Delta A \end{pmatrix} \tag{28}$$

$$\Delta X = \begin{pmatrix} \Delta P_{(3\times 1)} \\ \Delta R_{(3\times 1)} \end{pmatrix} \tag{29}$$

with the deviation errors ΔP along the axes x_0, y_0 and z_0. Similarly ΔR contrains the orientation errors about the axes x_0, y_0 and z_0.

5 THE OPTIMIZATION OF THE ERROR

5.1 The Position Error (EP)

The EP occurs when the tool deviates laterally of the desired weld line and contributes to positional inaccuracies. The error created along the normal of the workpiece during FSW does not affect the positional accuracy of the tool in the welding plane. But can be affect the welding quality then, the deviation errors creted along the three axes in the space have been minimized using the following expression:

$$EP = \sqrt{\Delta x^2 + \Delta y^2 + \Delta z^2} \tag{30}$$

With Δx, Δy and Δz are the deviation along the axis x_0, y_0 and z_0 respectively.

5.2 The Orientation Error (ER)

Among the FSW parameters we defined the tilt angle. In some applications, it is different from zero. And a higher value of this angle generates a blocking in advance, and a smaller value causes weld defects. Therefore, this angle has to be chosen with care, before starting the welding. In addition, it is very important that it remains constant during welding. But the action of the external loads changes the tool orientation which leads to an undesired tilt angle value and results an orientation error. Consequently, we get an incorrect welding. The orientation error reads:

$$ER = \sqrt{\Delta A^2 + \Delta B^2 + \Delta C^2} \tag{31}$$

5.3 Optimization Results

For a good quality of welding an optimization algorithm in MATLAB is developed that minimizes ER and EP. This has been done by optimization the following function:

$$E = (\lambda EP + ER)^2 \tag{32}$$

Where, λ is the Lagrange multiplier.

The position and the orientation errors are in terms of the parameters of the parallel structure which are defined with the matrix:

$$V = \begin{pmatrix} r_p \\ r_M \\ x_M \\ y_M \\ z_M \end{pmatrix}$$

Then, as previously mentioned r_p is the dimention of the platform, r_M is the dimention of the base, x_M, y_M and z_M are the coordinates of the base center O_M (see Fig. 2). In addition, these errors depend on the forces created by the three actuators of the parallel structure:

$$F_p = \begin{pmatrix} F_1 \\ F_2 \\ F_3 \end{pmatrix}$$

To minimize E, we developed an optimization algorithm in MATLAB. This algorithm calculated the optimal parameters which correspond to the minimum deviation. Thereafter this algorithm gives us the optimal three forces which have to be realized by the parallel structure as a fonction of the position of the tool during welding. These parameters and forces then correspond to a minimum error.

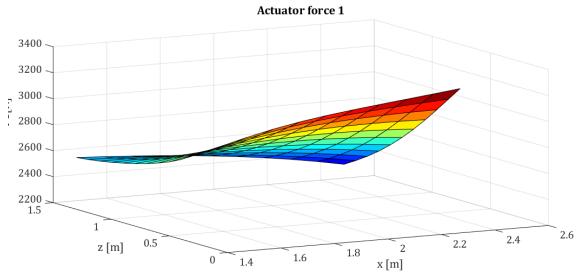

Figure 5: External force created by the limb 1 of the parallel structure.

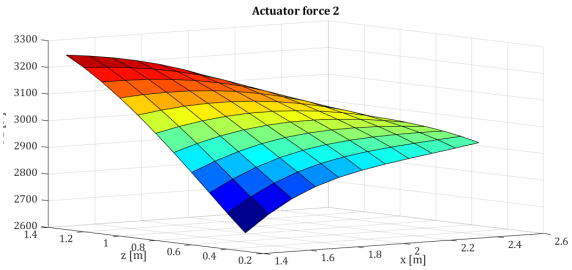

Figure 6: External force created by the limb 2 of the parallel structure.

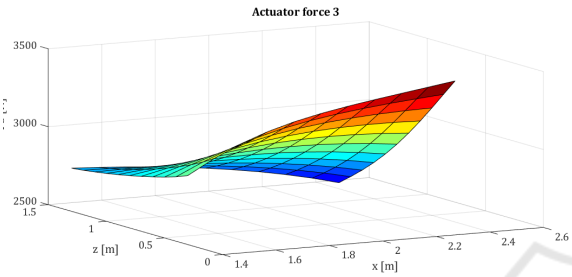

Figure 7: External force created by the limb 3 of the parallel structure.

It is revealed that F_2 is totally different from F_1 and F_3. However, F_1 has approximately the same value as F3 (see Fig. 5 and Fig. 7). As expected this is because F_2 is applied directly on the welding line while F_1 and F_3 are applied symmetrically on both sides of the welding line. Moreover, it has been observed that to correct the error, forces created by the parallel structure are between 2500 N and 3500 N.
Therefore the parallel structure is technically feasible.

The dimensioning parameters of the parallel structure and the three forces estimated to minimize the function E were used to calculate the position and rotation error. As shown in Fig. 8, the maximum rotational error is equal to 2.5×10^{-3} rad. Similarly, as shown in Fig. 9 the maximum position error is equal to 8×10^{-8} mm. The deviation of the tool is very well corrected by adding the parallel structure.

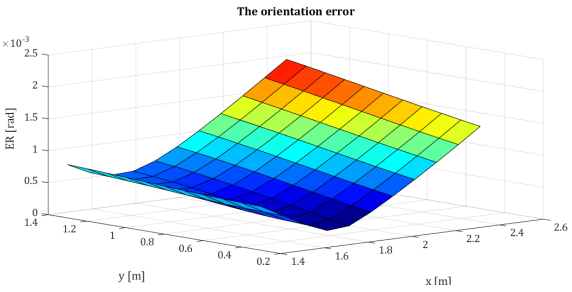

Figure 8: The orientation error (ER).

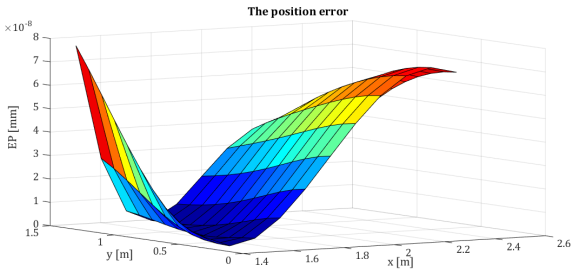

Figure 9: The position error (EP).

5.4 The Workspace of the Structure

The idea to add a parallel structure allows improving the rigidity of the robot. However, it limits the workspace and the index of the manipulability (De Backer, 2014). The workspace of the hybrid structure was not calculated in this work. However, it has been simulated using the software Catia. This simulation shows what happens by using a real system and how this system works in the face of real disturbances. Furthermore, From this simulation it has been observed that the tool can go up to $y_0 = \pm 1.2$m (because of the structure symmetry on the plane (x_0, z_0)). Further, different configurations have been tested in the plane $y_0 = 1.2$m using Catia as shown in Fig. 10. It has been revealed that there is no collision between the serial and the parallel structure in each configuration. At an initial stage, the workplace can be estimated by a parallelepiped of the following dimensions. the large length of the base equal 2.5m, the small length of the base equal 2.5m and the height equal 1m. To know the exact limits of the tool before collision it is necessary to calculate the workspace correctly.

6 CONCLUSIONS

The elasticity of industrial robots and limited force capability are barriers for achieve a successful robotic FSW which limits its use for high quality welding. Usually, this elacticity causes errors to follow the desired trajectory. There are two types of error; position error (EP) and orientation error (ER). These two errors are calculated in Cartesian space using the joint stiffness model, the kinematic and dynamic models of the manipulator. In this work a parallel structure was added to polyarticulated robot to minimize them. Optimization has been carried out using an algorithm developed in Matlab. The algorithm calculates the parameters of the parallel structural V and the three forces generated by this structure F_p to minimize the

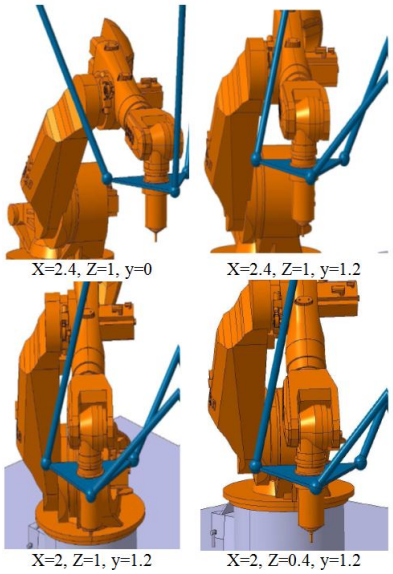

Figure 10: the workspace of the hybrid structure.

position and the orientation error during welding. For ours example we obtained a small orientation error of 0.1° and a very small position error of approximately zero.

Using the software Catia we estimated approximately the workspace of the serial and parallel robots by a parallelepiped. The volume of the parallelepiped equals $5.76m^3$.

With the proposed solution, the accuracy of positioning the tool and the FSW welding performance can be greatly improved. This assist device allows to improve the stiffness of an industrial robot. This approach allows us to gain in terms of stiffness, however, it limits the workspace. Moreover the main advantage of a serial robot is its workspace. But, despite this limitation of the application flexibility, this solution can ensure a process with good accuracy for simple paths and also for complex paths as the angle between the axis of the tool and the axis z_0 stays in the workspace of the hybrid structure. So finally, the structure can be useful for many industrial applications with the advantage of high welding quality.

ACKNOWLEDGEMENTS

The authors would like to thank the Doctoral School SMI of Arts et metiers ParisTech and the Institut of Technical Mechanics of KIT for their support.

REFERENCES

Balasubramanian, B. Gattu, R. S. M. (2009). Process forces during friction stir welding of aluminium alloys. 14:141–145.

Bres, A., Monsarrat, B., Dubourg, L., Birglen, L., Perron, C., Jahazi, M., and Baron, L. (2010). Simulation of friction stir welding using industrial robots. *Industrial Robot*, 37(1):36–50.

Chiaverini, S., Siciliano, B., and Villani, L. (1994). Force/position regulation of compliant robot manipulators. *IEEE Transactions on Automatic Control*, 39(3):647–652.

De Backer, J. (2014). *Feedback control of robotic friction stir welding*. PhD thesis, University west.

De Luca, A., Manes, C., and Ulivi, G. (1989). Robust hybrid dynamic control of robot arms. In *Decision and Control, 1989., Proceedings of the 28th IEEE Conference on*, pages 2641–2646. IEEE.

Deblaise, D., Hernot, X., and Maurine, P. (2006). A systematic analytical method for pkm stiffness matrix calculation. In *Robotics and Automation, 2006*, pages 4213–4219. Proceedings of the 2006 IEEE International Conference on Robotics and Automation.

Duelen, G. and Schröer, K. (1991). Robot calibration: method and results. *Robotics and Computer-Integrated Manufacturing*, 8. 4.

Dumas, C. (2011). *Développement de méthodes robotisées pour le parachèvement de pièces métalliques et composites*. PhD thesis, Université de Nantes.

ESAB (2013). Boeing selects esab for space launch system project. (2013, 2013/09/06).

Fuller 2007 (2007). *Friction Stir Welding and Processing*, chapter Chapter 2 Friction Stir Tooling: Tool Materials and Designs, Friction Stir Welding and Processing. ASM International. ISBN-13 978-0-87170-840-3.

Gibson, B., Lammlein, D., Prater, T., Longhurst, W., Cox, C., Ballun, M., Dharmaraj, K., Cook, G., and Strauss, A. (2014). Friction stir welding: process, automation, and control. *Journal of Manufacturing Processes*, 16(1):56–73.

Khalil, W. and Creusot, D. (1997). Symoro+: A system for the symbolic modelling of robots. *Robotica*, 15:153–161.

Khalil, W. and Kleinfinger, J. (1986). New geometric notation for open and closed-loop robots. pages 1174–1179.

Palpacelli, M. (2016). Static performance improvement of an industrial robot by means of a cable-driven redundantly actuated system. *Robotics and Computer-Integrated Manufacturing*, 38:1–8.

Qin, J., Leonard, F., and Abba, G. (2014). Nonlinear discrete observer for flexibility compensation of industrial robots. *IFAC Proceedings Volumes*, 47(3):5598–5604.

Raibert, M. and Craig, J. (1981). Hybrid position/force control of manipulators. *Journal of Dynamic Systems, Measurement and Control, Transactions of the ASME*, 103(2):126–133.

Schröer, K. (1993). Theory of kinematic modelling and numerical procedures for robot calibration. *Robot Calibration, Chapman & Hall, London*, pages 157–196.

Siciliano, B. and Khatib, O. (2016). *Springer handbook of robotics*. Springer.

Smith, B. C. (2007). *Friction Stir Welding and Processing*, chapter 11 Robots and machines for friction stir welding / processing, Friction Stir Welding and Processing. ASM International.

Soron, M. (2008). Towards multidimensionality and flexibility in fsw using an industrial robot system. *Welding in the World*, 52(9-10):54–59.

Strombeck, A., Schilling, C., and Santos, J. (2000). 2D and 3D friction stir welding with articulated robot arm. In *Proc. of 2nd International Friction Stir Welding Symposium*, Gothenburg, Sweden.

Thomas, W. M., Nicholas, E. D., Needham, J. C., Murch, M. G., Temple-Smith, P., and Dawes, C. J. (1991). International patent application pct/gb92/02203. Technical report, The Welding Institute, London, UK.

Voellner, G., Zaeh, M., Silvanus, J., and Kellenberger, O. (2007). Robotic friction stir welding. Technical report, SAE Technical Paper.

Wernholt, E. and Östring, M. (2003). Modeling and control of a bending backwards industrial robot. *Department of Electrical Engineering,Linköping, Sweden*, page 38.

Yoshikawa, T. (2000). Force control of robot manipulators. In *Robotics and Automation, 2000. Proceedings. ICRA'00. IEEE International Conference on*, volume 1, pages 220–226. IEEE.

Zaeh, M. F. and Voellner, G. (2010). Three-dimensional friction stir welding using a high payload industrial robot. *Production Engineering*, 4(2-3):127–133.